Method for Calculating the Potential Distribution of Nonlinear Ion Mirror and Modeling a Dust-Impact Mass Spectrometer

I. Piyakov [1], D. Rodin [2], M. Rodina [1]

[1] Department of design and technology of electronic systems and devices, Samara University, Samara, Russia
E-mail: m.a.rodina@yandex.ru
[2] Department of radioengineering, Samara University, Samara, Russia
E-mail: rodin@ssau.ru

Received: 09.11.2016

Abstract. Dust-impact mass spectrometers are used to analyze the chemical composition of micrometeoroids and space debris particles. The focusing of charged particles packets produced by high-speed interaction is complicated because of their high energy spread. The focusing can be achieved by using high voltages, or using electrical fields with special distributions. The method of analytical calculation of such nonlinear distribution is given in this paper. The nonlinear electrostatic ion mirror with a given distribution of potential provides the temporal focusing of ions with an energy spread of up to 25% of the accelerating voltage. To verify the focusing ability of the resulting potential distribution the trajectories of ions with different coordinates of origin and different initial energy spread were calculated. The mass resolution is calculated on the basis of ions trajectories and times of flight. The results of trajectories simulation allow us to conclude that nonlinear ion mirror provides sufficient level of temporal focusing to resolve simple substances such as aluminium, ferrum, lithium and other metals that can be detected in the chemical composition of micrometeoroids and space debris particles.

Keywords: dust-impact mass spectrometer; time of flight mass spectrometer; mass analyzer; nonlinear ion mirror; reflectron

INTRODUCTION

Time of flight mass spectrometers are widely used not only in laboratory but also for carrying out *in-situ* space experiments [1, 2]. The latter includes the scope of the study of outer space, the chemical composition of cosmic dust particles of natural and artificial origin, micrometeoroids and space debris particles. For such analysis of the chemical composition a dust-impact time of flight mass spectrometers are used, which principle of operation is based on the mechanism of impact ionization [3]. The advantages of time of flight mass spectrometer as compared to other mass analyzing devices are: small size, high sensitivity, and the ability to determine the composition of cosmic dust particles having a random nature of the interaction of particles with the target of the device. The use of ion mirrors in the design of the device improves the performance of the mass spectrometer by increasing the ion path length in the fieldless areas, as well as realization of the space-time focusing of the ion packets in the

detector plane [4, 5]. However, with the increase of the initial energy spread of ions (e.g., resulting from high-speed interaction of micrometeorite and target) the temporal error in focusing of ion packets is also increased, which limits the performance of this type of analyzers and requires the use of high accelerating voltage [6] or nonlinear potential distribution in reflector [7].

Analytical Expression for Ideal Focusing

The authors of [8] propose a method for calculating the distribution of the nonlinear axial potential electrostatic ion mirror, providing total independence of the drift time of the ions from their initial energy. The method is based on the fact that ions with different initial energy meet their unique reflection equipotentials, which longitudinal coordinates monotonically increase with the energy of the corresponding ions. Thus, the ions with higher energy have a longer path within the ion mirror, which compensates the initial energy spread of the ions.

Expression describing the desired potential distribution in the reflector can be written as the integral equation:

$$\Delta t(\Delta U) = 2\sqrt{\frac{m}{2q}}\int_0^{z^*}\frac{dz}{\sqrt{\Delta U - U}}, \qquad (1)$$

where m, q – mass and charge of ion; z – current longitudinal coordinate in the reflection area; z^* – coordinate of the turning point of ions; $q\Delta U$ – the initial energy of ions; U – potential in the area of reflection (entry point in this area corresponds to the zero potential), $\Delta t(\Delta U)$ – the difference in time of flight for $q\Delta U$ initial energy, which should be compensated.

Consider this method of calculation applied to the design of dust-impact mass spectrometer.

Structure of the Device and Desired Reflector Potential Distribution

Figure 1 shows the structure of dust-impact time of flight mass spectrometer with a nonlinear reflector. Dust particles at the speed of V_0 hit the target 1 and form a plasma cloud. Initially, the target has a potential equal to the accelerating voltage, the accelerating field separates the charged particles, ions are accelerated and get into nonlinear reflector, electrons are deposited on the target and form a current pulse amplified by the amplifier 5. This pulse turns off controlled pulsed voltage source 6 to remove accelerating field. Controlled pulsed voltage source 6 forms impulse to start recording. Ions reflect in the ion mirror and, as the accelerating voltage is already turned off, pass through the target, reflect in a parabolic reflector, pass through a spherical corrector and hit the detector 4.

Here 1 – a target with holes, 2 – flat grid, 3 – parabolic reflector, 4 – detector, 5 – electron pulse amplifier, 6 – accelerating voltage generator.

Time of flight of the ion with mass m and charge q for the path inside of the device, except the nonlinear reflector, can be written as following:

$$t_\Sigma(\Delta U) = \left\{\frac{2L_1}{U_1}\left(\sqrt{U_1+\Delta U}-\sqrt{\Delta U}\right)+\frac{2L_{fl}}{\sqrt{U_1+\Delta U}}+\right.$$

$$+\frac{4L_3\sqrt{U_1+\Delta U}}{kU_1}+\frac{4L_5}{U_1}\left(\sqrt{U_1+\Delta U}-\sqrt{\Delta U}\right)\Bigg\}, \tag{2}$$

where L_1 – length of accelerating gap; L_{fl} – length of fieldless areas; L_3 – distance between parabolic electrodes; L_5 – length of decelerating gap; U_1 – accelerating potential; ΔU – initial kinetic energy of ion.

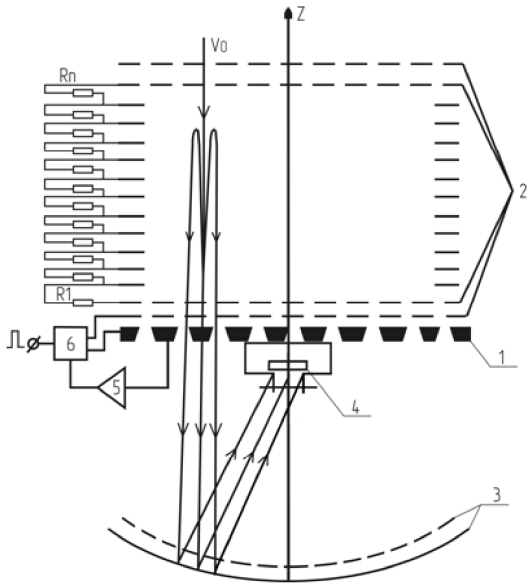

Figure 1. Structure of the device

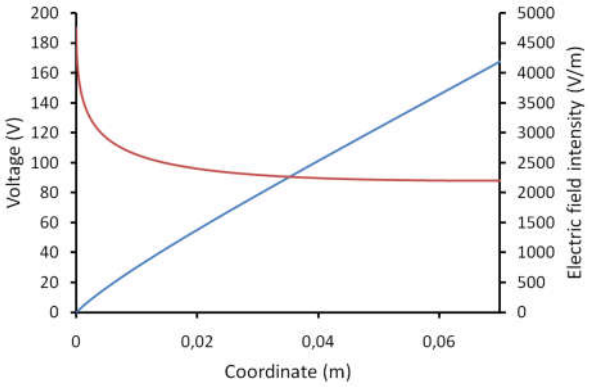

Figure 2. Desired distribution of potential (blue line) and field intensity (red line)

We can regroup summands in (2) to obtain coefficients for the different powers of ΔU:

$$C_0=\frac{t_\Sigma(0)}{\sqrt{m/2q}}=\frac{1}{\sqrt{U_1}}\left(2L_1+L_{fl}+\frac{4L_3}{k}+4L_5\right), \tag{3}$$

$$C_2=-\left(\frac{2L_1}{U_1}+\frac{4L_5}{U_1}\right), \tag{4}$$

$$C_2=\frac{2L_1}{U_1}+\frac{4L_3}{kU_1}+\frac{4L_5}{U_1}, \tag{5}$$

$$C_3=L_{fl}. \tag{6}$$

Thus, the expression describing time of flight difference will be the follows:

$$\Delta t_\Sigma(\Delta U)=\sqrt{\frac{m}{2q}}\left(C_0-C_1\sqrt{\Delta U}-C_2\sqrt{U_1+\Delta U}-C_3\frac{1}{\sqrt{U_1+\Delta U}}\right). \tag{7}$$

Solution of the equation (1) can be found trough integration:

$$z(U)=\frac{1}{2\pi}\int_0^U\frac{\Delta t_\Sigma(\Delta U)}{\sqrt{U-\Delta U}}d\Delta U. \tag{8}$$

Using expressions (3)–(6) and introducing:

$$u = \frac{U}{U_1}, \tag{9}$$

we can obtain inverse function, which describes dependence of longitudinal coordinates from potential inside the reflector:

$$z(u) = \frac{1}{2\pi}\left\{2C_0\sqrt{U_1 u} - \frac{\pi}{2}C_1 U_1 u - C_2 U_1\left(\sqrt{u} + (1+u)\arcsin\sqrt{\frac{u}{1+u}}\right) - \right.$$

$$\left. - 2C_3 U_1 \arcsin\sqrt{\frac{u}{1+u}}\right\}. \tag{10}$$

Resulting distributions of potential and electric field intensity are shown on Fig. 2, here the blue line is the potential distribution and the red line is the electric field intensity.

SYNTHESIS OF THE DESIRED REFLECTOR'S POTENTIAL DISTRIBUTION

Physical synthesis of the field with a given distribution of the axial potential by setting the potentials of the field defining elements according to the above expression is impossible. The larger inner diameter of the ring electrodes defining the field leads to greater difference of the field on the axis from the ideal distribution.

To solve the problem of the reflector field distribution synthesis, we have developed software for calculating potentials of field defining elements. This software uses genetic optimization algorithm and CUDA-accelerated library for Laplace equation solving. Each field distribution in population (a set of field defining potentials on electrodes) is being tested according to function of error minimization, the best specimens of the population are crossed and form a new generation. Functioning of the algorithm ends when the minimum error of the desired field structure synthesis is achieved.

Using the described software, we obtained the values of the field defining elements potentials, providing minimum synthesis error for the desired field distribution on the axis of the reflector. On the basis of the result set of potentials, two-dimensional distribution of the field inside the reflector was calculated, as well as the relative error of the synthesis on the axis and the periphery of the reflector. The two-dimensional potential distribution is shown in Fig. 3. The results of calculations are shown in Fig. 4.

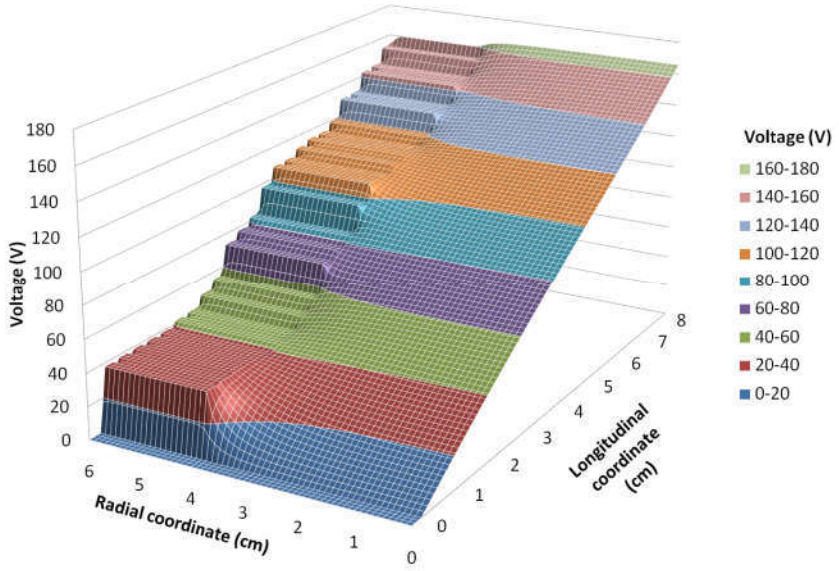

Figure 3. Potential distribution in the reflector

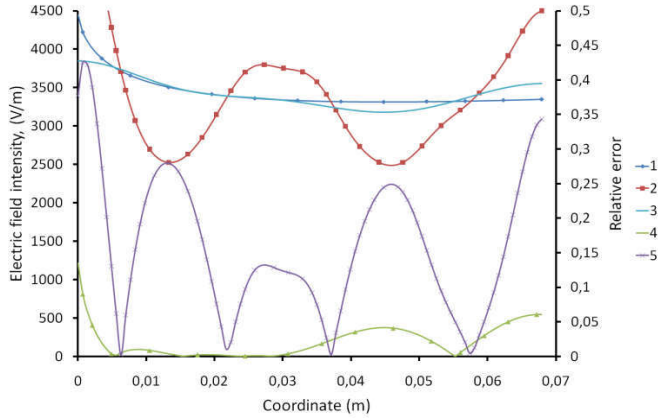

Figure 4. Electric field intensity and relative synthesis error: 1 – desired field, 2 – field on the axis of reflector, 3 – field on the periphery of the reflector, 4 – relative error on the axis of the reflector, 5 – relative error on the periphery of the reflector

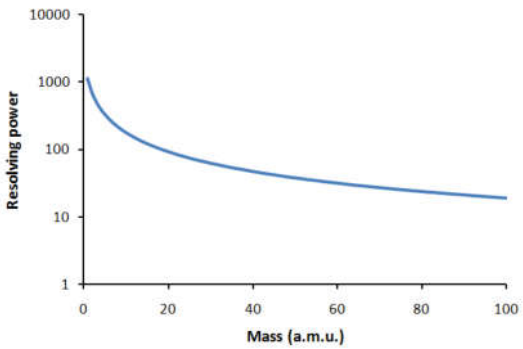

Figure 5. Dependency of the resolving power from the mass

IONS TRAJECTORIES SIMULATION AND DEVICE RESOLUTION

The ions trajectories were calculated using numerical Runge – Kutta integration method of fourth order. Maxwell velocity distribution in a given energy range is provided by using a special ion packets generator. The number of ions in the packet is selected based on the condition of smoothness of the velocities distribution. For each mass M_i mean time of flight was calculated:

$$T_{mean\ i} = \frac{1}{N}\sum_{j=1}^{N} T_j, \tag{11}$$

where T_j – individual ion in packet time of flight.

Root mean square deviation is determined according to the expression:

$$G_{T_i} = \sqrt{\frac{1}{N}\sum_{j=1}^{N}\left(T_j - T_{mean}\right)^2}. \quad (12)$$

And the resolution by sigma:

$$R_{G_i} = \frac{T_{mean\,i+1} - T_{mean\,i}}{2G_{T_i}}, \quad (13)$$

where G_{Ti} – root mean square deviation.

On the basis of the time of flight for the initial energy spread of 60 eV, the resolution from mass dependency was calculated, it is shown in Figure 5. Also dependence of resolving power from the radial coordinate of impact and initial energy spread of ions was calculated, which is shown in Table 1.

CONCLUSION

The results allow us to confirm the applicability of the described approach to the design of dust-impact time of flight mass spectrometers for space research with relatively high resolution (for a given accelerating voltage 250 V) in a wide range of initial energy spread of ions and impact coordinate. A further increase in resolution is possible by increasing the accelerating voltage (and thus reduce the relative energy spread of the ion packets), or by introduction to the design of the instrument of various modifications, such as additional compensating decelerating gaps and focusing ion lenses.

Table 1. Dependence of resolving power from the radial coordinate of impact and initial energy spread of ions

Radial coordinate of impact, mm	Initial energy spread, eV			
	15	**30**	**45**	**60**
0	1122	515	471	515
10	949	529	618	721
20	352	379	196	153
30	100	107	36	31

REFERENCES

1. Langevin, Y., Hilchenbach, M., Ligier, N., Merouhane, S., Hornung, K., & the COSIMA team (2015). Typology of dust particles collected by the COSIMA mass spectrometer in the inner coma of 67P/Churyumov Gerasimenko from Rendez-Vous to perihelion. *EPSC Abstracts, vol. 10*, 591–592.
2. Kempf, S., Altobelli, N., Briois, C., Grün, E., Horanyi, M., Postberg, F., Schmidt, J., Srama, R., Sternovsky, Z., Tobie, G., & Zolotov, M. (2014). SUDA: A dust mass spectrometer for compositional surface mapping for a mission to europa. *EPSC Abstracts, 9*, 229–230.
3. Hornung, K., Malama, Y. G., & Kestenboim, K. S. (2000). Impact vaporization and ionization of cosmic dust particles. *Astrophysics and Space Science, 274*(1–2), 355–363. doi:10.1023/A:102655350
4. Karataev, V. I., Mamyrin, B. A., & Shmikk, D. V. (1971). The new principle of ion packets focusing in time of flight mass spectrometry. *Zhurnal Tekhnicheskoi Fiziki, 41*(7), 1498–1501.
5. Kartaev, V. I., Mamyrin B. A., Shmikk, D. V., & Zagulin, V. A. (1973) The mass-reflectron, a new nonmagnetic time-of-flight mass spectrometer with high resolution. *Sov. Phys. – JETP, 37*(1), 45–48.
6. Sternovsky, Z., Amyx, K., Bano, G., Landgraf, M., Horanyi, M., Knappmiller, S., Robertson, S., Grün, E., Srama, R., & Auer, S. (2007). Large area mass analyzer instrument for the chemical analysis of interstellar dust particles. *Workshop on Dust in Planetary Systems*, September 26–30, 2005, Kauai, Hawaii, 205–208.

7. Austin, D. E., Ahrens, T. J., & Beauchamp, J. L. (2002). Dustbuster: a compact impact-ionization time-of-flight mass spectrometer for *in situ* analysis of cosmic dust. *Review of Scientific Instruments, 73*(1), 185–189. doi:10.1063/1.1427762

8. Rodin, D. V., Semkin, N. D., Piyakov, I. V., & Pomelnikov, R. A. (2012) Analytical method for computing the electrostatic field distribution in the reflector of the time-of-flight mass spectrometer. *Technical Physics, 57*(10), 1400–1405. doi:10.1134/S1063784212100192